

# A flux emergence model for solar eruptions

V. Archontis<sup>1</sup> and A.W. Hood<sup>1</sup>

## ABSTRACT

We have simulated the 3D emergence and interaction of two twisted flux tubes, which rise from the interior into the outer atmosphere of the Sun. We present evidence for the multiple formation and eruption of flux ropes inside the emerging flux systems and hot arcade-like structures in between them. Their formation is due to internal reconnection, occurring between oppositely directed, highly stretched and sheared fieldlines at photospheric heights. Most of the eruptions escape into the corona, but some are confined and fade away without leaving the low atmosphere. As these flux ropes erupt, new reconnected fieldlines accumulate around the main axis of the initial magnetic flux systems. We also show the complex 3D fieldline geometry and the structure of the multiple current sheets, which form as a result of the reconnection between the emerging flux systems.

*Subject headings:* Sun: magnetic fields, Sun: corona, MHD

## 1. Introduction

Partial eruption of a flux rope can be produced by favourable, *imposed* shearing motions at the photosphere. This shearing can occur as sunspots with opposite polarity move apart along the neutral line of an active region. Then, as the rising magnetic system expands, the sheared magnetic fieldlines are stretched and undergo internal reconnection, at low heights, which leads to partial eruption of magnetic flux (Manchester et al. 2004). This is consistent with the ‘tether-cutting’ mechanism (Sturrock 1989; Moore et al. 2001), in which, effective reconnection of magnetic fieldlines at the core of a magnetic bipole releases the energy stored in the sheared field, resulting in an eruption. An important factor in determining whether an emerging flux rope will erupt is the amount of twist of the fieldlines around the central axis of the tube (Murray et al. 2006). If the winding of the fieldlines is high enough, a kink instability occurs that eventually leads to either a confined or an ejective eruption (Török & Kliem 2005; Gibson & Fan 2006).

---

<sup>1</sup>School of Mathematics and Statistics, University of St Andrews, North Haugh, St Andrews, Fife KY16 9SS, UK

Observations (Sterling & Moore 2004, 2005; Jiang et al. 2007) have shown active-region filament eruptions when new flux emerges near the location of a preexisting emerging flux region. It is likely that the new emergence is important in the eruption onset. Several numerical models, requiring multipolar magnetic configurations for eruptions, have reproduced the above and similar-like observations. In the breakout model (Antiochos 1998), a sheared bipole rises into an overlying bipole and ‘external’ reconnection occurs at a magnetic null point at their interface. When the reconnection becomes fast enough the rising bipole breaks through the ambient field and erupts.

Another possibility, shown in magnetofrictional simulations, is that flux ropes are formed and erupt due to slow diffusion of decaying flux from active regions, which interact through converging motions on the photosphere (MacKay & van Ballegoijen 2006; van Ballegoijen & MacKay 2007). Also, Chen & Shibata (2000) simulated the interaction between a flux system with a detached flux rope and an emerging flux system that appears to one side of the primary field. Reconnection between the flux systems leads to a vertical current sheet below the detached flux rope, which eventually experiences a fast ejection.

In this Letter, we consider the 3D extension of the model by Archontis, Hood & Brady (2007) (hereafter called AHB model) in which one (leading) flux tube rises through a stratified atmosphere to create a coronal field for the second (following) tube to rise into. The 3D model simulates: 1) the intricate reconnection of the two flux systems 2) the multiple eruptions of flux ropes, which are initiated by the new emergence of flux and 3) the formation of current sheets and hot arcade structures.

## 2. Model

The initial stratification of the stratified atmosphere and the properties of the magnetic flux tubes are similar to the AHB model. The simulations use a 3D version of the Lare shock-capturing code (see Arber et al. (2001)). The time-dependent, resistive and compressible MHD equations are solved by a Lagrangian remap scheme, including uniform gravity. The energy equation is adiabatic and includes viscous and Joule dissipation terms. The resistivity is enhanced at sites where the current density exceeds a certain value in a similar manner to the AHB model. At the beginning of the experiment two flux tubes are located 2.9Mm and 2.2Mm below the photosphere, with axes parallel to the  $y$  direction. The fieldlines are uniformly twisted around the main axis of each tube. The initial twist is such that the tubes are stable to the kink instability. Both tubes are left-handed and can reconnect when they come into contact. The rising motion of the tubes is triggered by a density excess along their central axes. The density deficit is reduced away from  $y = 0$  following a Gaussian profile,

similar to the experiment by Archontis et al. (2005). The length scale of the buoyant part of the tubes is defined by the parameter  $\lambda$ , where  $\lambda = 20$  in our experiments. This deficit makes the tubes less dense and more buoyant in the middle part of their axes. As they rise through the solar interior, they form  $\Omega$ -shaped loops due to magnetic buoyancy.

All variables are made dimensionless against their photospheric values, namely: pressure,  $P = 1.4 \cdot 10^5 \text{ erg cm}^{-3}$ ; density,  $\rho = 3 \cdot 10^{-7} \text{ g cm}^{-3}$ ; temperature,  $T = 5.6 \cdot 10^3 \text{ K}$ ; scale height,  $H = 170 \text{ km}$ ; time,  $t = 25 \text{ sec}$ ; velocity,  $V = 6.8 \text{ km sec}^{-1}$  and magnetic field,  $B = 1.3 \cdot 10^3 \text{ Gauss}$ . The dimensionless coordinates are  $(-100 \leq x \leq 100)$ ,  $(-100 \leq y \leq 100)$  and  $(-10 \leq z \leq 140)$ . The stratified atmosphere includes the top of the solar interior from  $z = -10$  to 22, two isothermal layers ( $z = 22$  to 32 for the photosphere and  $z = 42$  to 140 for the corona) and a *transition region* with a steep temperature gradient joining them. The size of the grid used in the numerical experiments is  $(256, 256, 320)$  points in the  $(x, y, z)$  directions, with  $x$  being the transverse coordinate and  $z$  the vertical coordinate.

### 3. Results and Discussion

The initial evolution of the system is similar to the evolution in the AHB model. When the leading tube reaches the photosphere a bipolar region is formed with a north-south orientation due to the initial strong twist of the fieldlines. Eventually, the bipolar region moves towards an east-west direction as more internal magnetic layers rise to the photosphere and the inclination of the anchored flanks of the tube becomes more vertical. After  $t = 35$ , the leading tube rises into the non-magnetized corona where it expands and *creates an ambient field* for the following tube to rise into. The direction of the fieldlines and the field strength vary away from the center of the expanding volume of the leading system and, thus, the newly formed ambient field is more complex than in the previous simulations of the interaction between an emerging field and a uniform coronal field.

As the newly emerged bipolar magnetic field is moving in opposite directions along the neutral line, shearing of the field occurs so that the magnetic field lines lose their strong azimuthal nature and run nearly parallel to the neutral line. Observations have shown that most bipolar sheared magnetic fields in active regions can produce ejective explosions such as flares and CMEs (Falconer 2001). Also, in our simulations the twisted and sheared magnetic field adopts an overall *sigmoidal shape* with two oppositely curved *elbow-like* regions at the two (east and west) ends of the neutral line (as illustrated in Fig. 1, left panel). The neutral line is stretched along the middle of the sigmoidal structure while the elbows are found on either side. During the evolution of the system, the curved region of the elbows consist of expanding loops of fieldlines that rise in opposite (north-east and south-west) directions.

The parts of the elbows close to the middle of the sigmoid, shear past each other and are ready to reconnect if they come into contact. This magnetic field configuration with the elbow-like structures has been reported in observations of solar eruptive events by Moore et al. (2001).

When the second flux system emerges at  $t \approx 40$ , a thin, curved, sheet-like current structure (Fig. 1, middle panel) is formed just above the top layers of the following tube and parallel to the interface of the magnetic flux systems, along the  $y$ -direction. An interesting result is that already at this early stage of the interaction, *asymmetry* is introduced into the system (Fig. 1, left panel) by the 3D nature of the fan-like expansion of the field. On the west side of the emerging regions, the fieldlines of the rising systems make a contact angle which is larger than on the east side, leading eventually to a higher current concentration and more efficient reconnection at the west side of their interface.

In a similar manner to the 2.5D AHB model, soon after the build up of the interface current concentration *plasmoid-like* structures develop inside the sheet. Due to the asymmetry, they are formed firstly towards the west side of the current sheet. The cool and dense plasmoids grow and are ejected upwards and sideways, as in the AHB model, allowing reconnection in the diffusion regime to occur at a *faster rate*.

Two new flux systems are formed by the reconnected fieldlines (Fig. 1, middle panel). At the *upper end* of the current sheet, reconnection forms an overlying field that joins the two emerging systems externally, mainly from the north-west side of the leading system to the south-east side of the following system while it spreads out mostly above the west sides of the emerging systems. At the start of the reconnection, the overlying field links the west-side flank of the leading tube with the east-side flank of the following tube. At the *lower end* of the current sheet, reconnection forms a series of magnetic loops in between the two emerging systems. The configuration of the low-lying magnetic loops is an *arcade-like* structure joining the leading and following tubes and is reminiscent of *post-flare loops*. The arcade is stretched and curved along the  $y$ -direction and grows in size as reconnection proceeds and more fieldlines are added to the top of the arcade. The temperature here could be as high as 2 MK. The arcade brightens when high velocity reconnection outflows, which carry hot material ejected from the current sheet, compress the plasma at the upper part of the arcade and increase the temperature.

During this time, due to the emergence of the leading tube the inner fieldlines are sheared horizontally and stretched vertically. Hence, oppositely directed fieldlines, which are rooted to the sigmoidal neutral line, are forced into contact. This internal reconnection of fieldlines is similar to the ‘tether-cutting’ mechanism (Moore & Roumeliotis 1992). In experiments with a single emerging tube, with the same initial properties, we find that internal ‘tether-

cutting’ reconnection occurs at  $t \approx 180$ . In the experiment with two emerging bipoles it occurs much earlier at  $t \approx 135$ .

In the model with the two tubes, reconnection occurs first (externally) at X-type points at the ends of the interface current sheet. At the lower end of the current sheet, the hot reconnected fieldlines form an arcade structure. The magnetic pressure inside this new arcade increases as reconnection proceeds and eventually exceeds the magnetic pressure of the leading flux system. Thus, the arcade expands sideways and pushes the south side of the leading system towards its neutral line. It is the combination of shearing along the neutral line, stretching due to expansion and the increasing magnetic pressure force of the arcade structure that leads to internal reconnection of the fieldlines just above the neutral line of the leading emerging system.

As the two emerging flux tubes continue to rise and interact, internal reconnection occurs at *many positions along the neutral line* of the leading magnetic flux system. Due to internal reconnection, *flux-rope-like structures* are formed inside the magnetized volume of the leading tube. Eventually, the ropes rise and erupt into the outer atmosphere. The eruption is due to the vigorous sideways pressure by the fast expanding arcade and the release of the magnetic tension force of the overlying field, after the ejection of the plasmoids out of the interface current sheet.

A striking result is that the eruptions produced in our simulations *do not appear simultaneously*. Also, multiple eruptions can be triggered from the same location inside the expanding volume of the leading system. As an example, the first formation and eruption of a *flux rope* occurs on the south-west part of the neutral line. This part of the leading tube is closer, due to the asymmetry mentioned above, to the following tube. Thus, the dynamical rearrangement of the magnetic field due to reconnection occurs faster at this region of the leading emerging tube. In general, the eruptions occurred in our experiment follow the direction of the overall 3D expansion of the emerging systems, which for the south-west side is preferentially the direction towards the following tube and for the north-east side is the opposite direction. Thus, the eruption of the first flux rope is directed towards the south side (Fig. 1, right panel). It is a confined eruption, being trapped between the envelope field of the leading tube and the expanding field of the upcoming tube that halts the further rise of the flux rope. Other eruptions, which occur at later stages of the evolution of the emergence, are more dynamic and seem to fully escape from the corona, in a *CME-like* manner. These eruptions are mainly directed towards the north side of the leading magnetic flux system.

The time evolution of the flux ropes formed *inside* the leading region, can be followed by locating the center (or *O-point*) of the ropes at various  $xz$  cross-sections (different values of  $y$ ) as functions of time. The height-time relation for 6 values of  $y$  is shown in the top

panel of Fig. 2. The bottom panel is the projection of their motion onto an  $xz$  slice. The confined eruption of the first flux rope is shown by the lines at  $y = -20$  and  $y = -10$ . The center of the rope for  $y = -20$  is lower than at  $y = -10$  at all times.

There are *two phases* during the eruption of the ropes. In the first, the flux ropes are moving with moderate speeds, while in the second they are accelerated towards the outer atmosphere. These curves are qualitatively similar to the time profiles of filament heights shown in the observations by Sterling & Moore (2004, 2005). We also estimate the temperature and current density in the area below the central part of the erupting flux ropes where a vertical current sheet is formed due to internal reconnection. We find that there is a slow increase in the first phase, which is followed by an intensity increase over the period of the fast eruption. The peak of the temperature and current density occurs when the fast rise is well underway. Since both quantities follow the same time evolution, it is likely that the reason for the change in the rise phase of the eruption is that reconnection is slower at the beginning but becomes faster, and operates with a higher growth rate, as the ropes rise. These results are also consistent with the observations mentioned above in which soft X-ray emission is found to occur during the slow-rise phase of a filament’s eruption and hard X-ray bursts occurred after the start of the fast eruption.

As shown above, the first formation of a flux rope and its eruption occurs in the southwest part of the leading tube. Figure 2 (bottom panel) shows that a secondary formation and eruption occurs at the same location ( $y=-10$ , dashed-triple dotted line), starting at  $t=145$ . Thus, *at least two eruptions are triggered from the same location* within the leading emerging system until the end of the simulation. Further eruptions may be triggered inside the expanding magnetized volumes since the system of the interacting bipoles does not reach an equilibrium but evolves dynamically. As the flux ropes erupt, they grow in radial extent as additional fieldlines reconnect at the vertical current sheet beneath them. The magnetized plasma inside the erupting ropes is a mixture of cold and hot plasma. The cold and dense plasma comes from the low atmosphere and is carried upwards by the tether-cutting reconnection forming concave upwards fieldlines. The hot plasma (up to 2 MK) is emitted inside the envelope of the rope by the reconnection jet, which blasts from the upper end of the vertical current sheet below the rope. The velocity at the center of the rope is  $\approx 10\text{-}15\text{ Km/sec}$ . However, the maximum upward velocity inside the complete volume of the rope reaches values up to 150 Km/sec, mainly due to the emission of the reconnection jet. The rising motion of the flux rope can result in a CME-like eruption.

Figure 3 (left panel) shows the temperature distribution in a vertical plane and magnetic fieldlines, which are traced from near the axis of the flux rope. The cold plasma is mostly concentrated near the axis of the flux rope while the hot plasma is overlying the axis on the

right side of the eruption. The fieldlines near the axis of the rope come from *both of the emerging flux systems*. More precisely, fieldlines from the following tube joins the leading tube, through the arcade structure between them before forming the erupting flux rope. These fieldlines undergo multiple reconnection events along their lengths and, thus, may end up in either of the flanks at the east-side boundary. The middle panel in Fig. 3 shows isosurfaces of current density, which are overplotted on the same set of fieldlines. A striking result is that long and twisted sheets are found close to the core of the erupting flux rope. In addition, arch-like current sheets that are less twisted and have different orientation to each other, are formed in the region between the emerging systems (see ‘A’ and ‘B’ in the figure). These structures, with enhanced current density, may be quasi separatrix layers. The right panel in Figure 3 is a blow-up of the region at the vertical current sheet below the erupting flux rope shown in the left panel. The fieldlines shown in the figure have been traced from the lower end of the vertical sheet. These are reconnected fieldlines that surround the leading flux tube’s original axis. Thus, the field below the vertical current sheet forms a tightly wound flux tube with its axis lying parallel to the neutral line of the leading bipolar region. The temperature rises up to 0.2 MK at the bottom of the current sheet, as hot reconnected plasma moves downward from the sheet. These fieldlines are also linked: a) to fieldlines that envelope the erupting flux rope from the north side (two fieldlines on left side of figure) and b) to fieldlines that form the hot arcade structure between the emerging flux systems.

Our 3D simulations show that the interaction of emerging flux tubes may lead to multiple eruptions of flux ropes. A network of twisted current sheets, with an overall S-shaped configuration, and hot cusp-like, arcade structures are also formed during the evolution of the system.

Computational time on the Linux clusters in St. Andrews (STFC and SRIF funded) are gratefully acknowledged.

## REFERENCES

- Antiochos, S.K. 1998, ApJL, 502, L181
- Arber, T. et al. 2001, JCoPh, 171, 151
- Archontis, V.; Hood, A. W. & Brady, C., 2007, A&A, 466, 367
- Archontis, V. et al. 2005, ApJ, 635, 2
- Chen, P.F. & Shibata, K., 2000, ApJ, 545, 524

- Falconer, D.A. 2001, JGR, 106, 25185
- Gibson, S. & Fan, Y., 2006, ApJ, 637, L65
- Jiang, Y-C. et al. 2007, CJAA, 7, 129
- Mackay, D. H. & van Ballegooijen, A. A., 2006, ApJ, 641, 577
- Manchester, W.IV. et al. 2004, ApJ, 610, 588
- Moore, R.L. et al. 2001, ApJ, 552, 833
- Moore, R.L. & Roumeliotis, G., 1992, Eruptive Solar Flares. Proceedings of IAU Colloquium 133.
- Murray, M.J. et al. 2006, A&A, 460, 909
- Sturrock, P.A. 1989, Solar Physics, 121, 387
- Sterling, A.C. & Moore, R.L., 2004, ApJ, 613, 1221
- Sterling, A.C. & Moore, R.L., 2005, ApJ, 630, 1148
- Török, T. & Kliem, B., 2005, ApJ, 630, L97
- van Ballegooijen, A. A. & Mackay, D. H., 2007, ApJ, 659, 1713



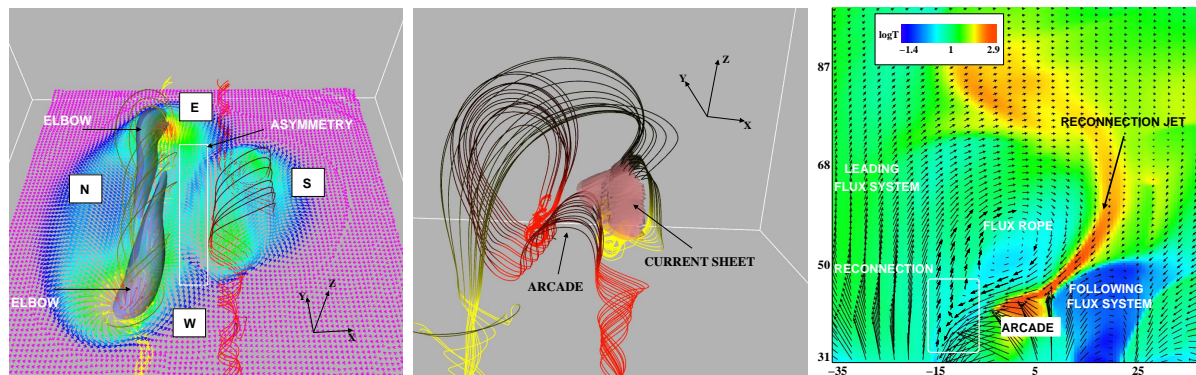


Fig. 1.— *Left:* Visualization of the full magnetic field vector (arrows) at photospheric heights, at  $t = 130$ . Also shown is fieldlines of the emerging tubes and isosurfaces of current density. The region around the asymmetry is underlined by the inset in the figure. *Middle:* Fieldline topology around the current sheet at the interface at  $t = 135$ . The darkest the color the weakest the magnetic field is along the fieldlines. *Right:* Confined eruption of a flux rope at  $t = 140$ . Superimposed is the magnetic field vector (arrows) in a vertical plane at  $y = -22$ . Sites of internal reconnection are shown in the inset rectangle of the panel.

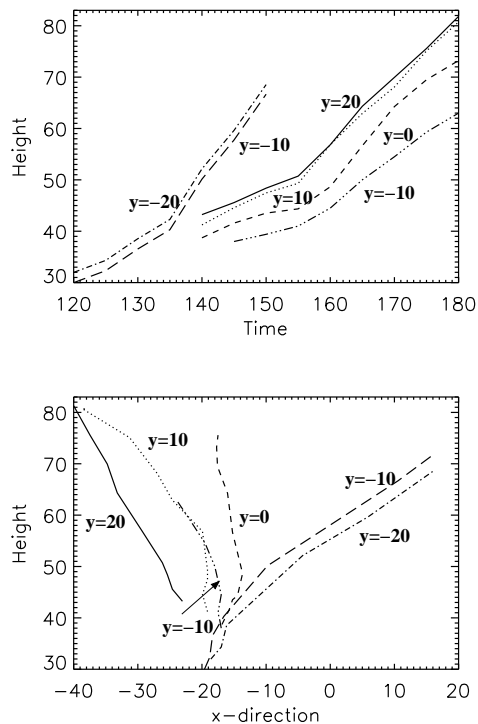


Fig. 2.— *Top*: Height-time relation of the centers of the flux ropes. *Bottom*: Projection of the rising motion of the centers of the flux ropes on a horizontal plane.

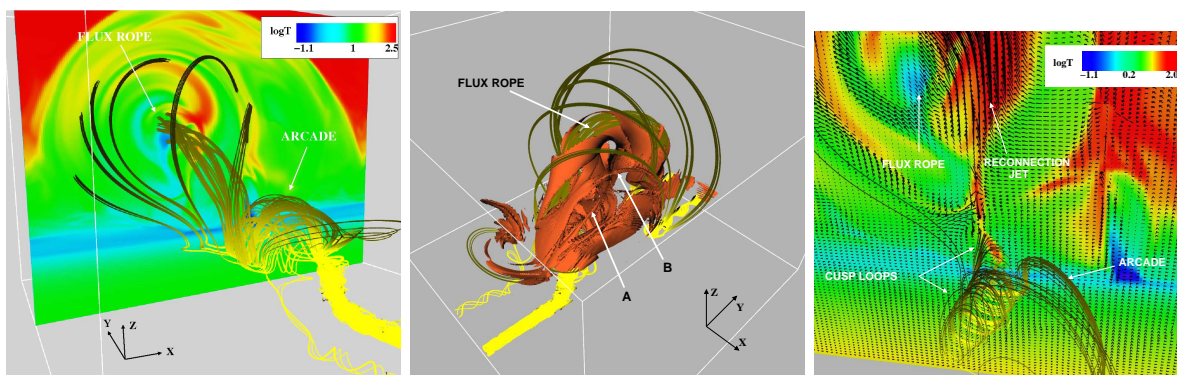


Fig. 3.— *Left*: Ejective eruption of a flux rope at  $t = 175$ . The temperature contours are on the plane  $y = 20$ . *Middle*: The same as in the left panel with isosurfaces of current density superimposed. *Right*: 3D visualization of fieldlines in the region below the erupting flux rope. Superimposed on the temperature contours is the velocity field (arrows) on  $y = 20$ .